npj | climate and atmospheric science

www.nature.com/npjclimatsci

ARTICLE OPEN

Check for updates

Insights from ozone and particulate matter pollution control in New York City applied to Beijing

Jie Zhang[1]✉, Junfeng Wang[2]✉, Yele Sun[3], Jingyi Li[2], Matthew Ninneman[4], Jianhuai Ye[5], Ke Li[2], Brian Crandall[6], Jingbo Mao[7], Weiqi Xu[3], Margaret J. Schwab[1], Weijun Li[8], Xinlei Ge[2], Mindong Chen[2], Qi Ying[9], Qi Zhang[10] and James J. Schwab[1]✉

Strict emission control policies implemented in two megacities of New York City (NYC) and Beijing show impacts on the non-linear relationship of their ozone (O_3) and fine particulate matter ($PM_{2.5}$) during summertime. Here we show these non-linear O_3-$PM_{2.5}$ relationships including a positive linear part reflecting the O_3/$PM_{2.5}$ co-occurrence and a negative power function part reflecting the O_3 formation suppression by $PM_{2.5}$ based on the multiyear surface observations. The control policies targeting sulfur dioxide and $PM_{2.5}$, then volatile organic compounds and nitrogen oxides, changed the $PM_{2.5}$ chemical composition which resulted in an increased linear slope that indicates a weaker O_3 control effect than occurred for $PM_{2.5}$. These policies also enhanced the relative $PM_{2.5}$ suppression effect as shown by an increase in the power function coefficient. Model simulations suggest that regional equal percentage emission reductions for Beijing and other Chinese megacities will be necessary to avoid further increase in the O_3/$PM_{2.5}$ linear slope and continuing occurrences of high levels of ozone.

npj Climate and Atmospheric Science (2022)5:85 ; https://doi.org/10.1038/s41612-022-00309-8

INTRODUCTION

Enhanced concentrations of ozone (O_3) and/or fine particulate matter ($PM_{2.5}$, particles with aerodynamic diameters <2.5 μm) adversely affect human health[1–3], and have been a wide concern in densely populated megacities[4–6]. They frequently co-occur during summer (June-August), which is due in part to stagnant meteorological conditions accompanied with high solar radiation and temperature under which high concentrations of nitrogen oxides (NO_x) and volatile organic compounds (VOCs) enhance $PM_{2.5}$ and O_3 formation[1,4].

Previous studies have demonstrated a positive relationship between the maximum daily 8-h average (MDA8) O_3 and the daily 24-h average (hereafter: DA24 in this study for simplification) $PM_{2.5}$ concentrations in polluted regions during summertime[5,6]. A maximum turning point (MTP) in the relationship of MDA8 O_3 versus DA24 $PM_{2.5}$ was observed at about 50~60 μg m^{-3} of DA24 $PM_{2.5}$ for Chinese megacity-clusters[6]. The MDA8 O_3 was linearly and positively correlated with DA24 $PM_{2.5}$ when DA24 $PM_{2.5}$ below MTP while it remained relatively stable despite the increasing $PM_{2.5}$ above the MTP. These changes have been attributed to the scavenging of hydroperoxyl (HO_2) and/or nitrate radicals (NO_3) by high concentrations of $PM_{2.5}$ that inhibited the photochemical production of O_3[7–9].

New York City (NYC) and Beijing are two megacities that have been extensively studied during the last two decades[10–12]. Strict emission control policies have been implemented in NYC since the 1970s with amendments in 1990 (https://www.epa.gov/clean-air-act-overview) and in Beijing from 2013[13], leading to substantial decreases in $PM_{2.5}$. Maximum O_3 concentrations have reduced more slowly than $PM_{2.5}$ in NYC[14], while they have increased in Beijing[15–18]. This discrepancy between $PM_{2.5}$ and O_3 following the imposition of emission controls at these two locations requires further investigation. To explore these, we analyzed the relationship of MDA8 O_3 and DA24 $PM_{2.5}$ by using 19 years of surface measurements in NYC and 6 years of measurements in Beijing, along with related aerosol chemical composition measurements. The features of the O_3-$PM_{2.5}$ relationships and their responses to emission controls in the two megacities are compared, empirically fit using a non-linear power function, and used as a basis for model calculations aimed at developing a future strategy for controlling $PM_{2.5}$ and O_3 together in Beijing and other Chinese megacity-clusters.

RESULTS

Dependence of the NYC O_3–$PM_{2.5}$ relationship on aerosol composition

Based on the magnitude of DA24 $PM_{2.5}$ concentration, the summertime periods of 2001-2019 were separated into 4 subperiods (Fig. 1a, $SP_{NY}1$: 2001-2003, $SP_{NY}2$: 2004-2008; $SP_{NY}3$: 2009–2013, $SP_{NY}4$: 2014-2019. See Data availability for the data sources). The standard deviation of the annual summertime average DA24 $PM_{2.5}$ in each period was below 1 μg m^{-3}. The relationship between MDA8 O_3 and DA24 $PM_{2.5}$ for each subperiod was developed (Fig. 1b) following the approach in Li et al.[6] and Buysse et al.[9] with the $PM_{2.5}$ data being binned in increments of 5 μg m^{-3}, and these relationships were fitted using a non-linear function including (1) a positive linear part reflecting

[1]Atmospheric Sciences Research Center, University at Albany, State University of New York, Albany, NY 12203, USA. [2]Jiangsu Key Laboratory of Atmospheric Environment Monitoring and Pollution Control, School of Environmental Science and Engineering, Nanjing University of Information Science and Technology, Nanjing 210044, China. [3]State Key Laboratory of Atmospheric Boundary Layer Physics and Atmospheric Chemistry, Institute of Atmospheric Physics, Chinese Academy of Sciences, Beijing 100029, China. [4]School of Science, Technology, Engineering and Mathematics, University of Washington Bothell, 18115 Campus Way NE, Bothell, WA 98011, USA. [5]School of Environmental Science & Engineering, Southern University of Science and Technology, Shenzhen 518055, China. [6]New York State Department of Environmental Conservation, Albany, NY 12233, USA. [7]Shanghai Key Laboratory of Atmospheric Particle Pollution and Prevention (LAP3), Department of Environmental Science and Engineering, Fudan University, Shanghai 200438, China. [8]Department of Atmospheric Sciences, School of Earth Sciences, Zhejiang University, Hangzhou 310027, China. [9]Department of Civil and Environmental Engineering, Texas A&M University, College Station, TX 77843, USA. [10]Department of Environmental Toxicology, University of California, Davis, Davis, CA 95616, USA.
✉email: jzhang35@albany.edu; wangjunfengnuist@163.com; jschwab@albany.edu

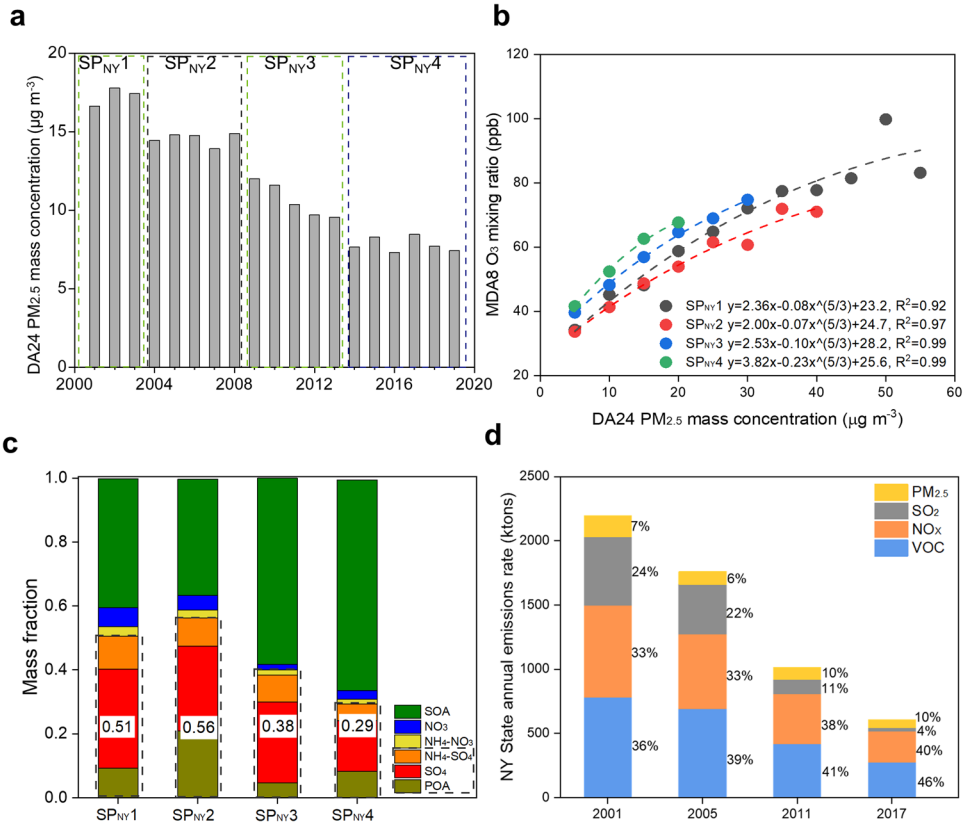

Fig. 1 O_3 and $PM_{2.5}$ in NYC. a The time series of the annual summertime average DA24 $PM_{2.5}$ in NYC for each subperiod specified in the main text; **b** NYC O_3-$PM_{2.5}$ relationship for the different subperiods with the non-linear fitting; **c** the aerosol mass fraction for each subperiod in NYC based on the AMS measurement from the representative year (Black dash box indicates SAP compounds. The number in each column indicates the SAP mass fraction); **d** the VOC, NO_x, SO_2, and primary $PM_{2.5}$ emissions of NY state in 2001, 2005, 2011, 2017.

their co-occurrence mainly due to their common precursors, e.g., NO_x and VOCs[19] and (2) a negative power function part reflecting the O_3 formation suppression by $PM_{2.5}$ through the uptake of HO_2/NO_2 by $PM_{2.5}$[7–9] and the reduced photolysis rates with $PM_{2.5}$ increasing[20] (Method 1). As shown in Fig. 1b, the O_3-$PM_{2.5}$ linear slope increased from around 2.0 during $SP_{NY}1$ and $SP_{NY}2$ to ~3.86 during $SP_{NY}4$, which corresponds to lower $PM_{2.5}$ mass concentration at the same O_3 pollution level comparing $SP_{NY}4$ to $SP_{NY}1$/$SP_{NY}2$, and also matched the discrepancy of the trends MDA8 O_3 and DA24 $PM_{2.5}$ extreme concentrations (the top5%) of each year (Supplementary Fig. 1a). The extreme concentrations decreased from 2001 to 2019 at a rate of 1.1 ppb yr^{-1} for MDA8 O_3 and 1.9 μg m^{-3} yr^{-1} for DA24 $PM_{2.5}$ (Supplementary Fig. 1a), corresponding to a total reduction of 22% and 62% for O_3 and $PM_{2.5}$, respectively. A larger O_3-$PM_{2.5}$ linear slope indicates a weaker control effect for O_3 than for $PM_{2.5}$.

Given that sulfate related inorganic and primary organic chemical components of $PM_{2.5}$ (e.g., sulfate, ammonium from ammonium sulfate, primary organic aerosol, hereafter SAP as the sum of these three components) do not share the NO_x and VOCs precursors with O_3, we divided the $PM_{2.5}$ composition into two groups: (1) the SAP, and (2) the non-SAP - with NO_x and VOCs as precursors (non-SAP: the sum of secondary organic aerosol (SOA), nitrate and nitrate-related-ammonium). The measured historical PM_1 chemical composition in the NYC metropolitan area (Method 2) shows a reduced mass fraction of SAP from 51% in $SP_{NY}1$ to 29% in $SP_{NY}4$ (Fig. 1c), consistent with the increased O_3-$PM_{2.5}$ linear slope (Fig. 1b). By excluding the influence of this change in SAP mass fraction, the differences in O_3-$PM_{2.5}$ slopes among the four subperiods were much smaller (Supplementary Fig. 1b). This demonstrates that the reduced SAP mass fraction can explain the increased O_3-$PM_{2.5}$ slope in NYC during the last two decades. The increased fraction of NO_x + VOCs in the total emissions ($PM_{2.5}$, SO_2, VOCs and NO_x) from 69% in 2001 to 85% in 2017 (Fig. 1d) means higher NO_x and VOCs emissions per ton of total emissions, which will lead to the relatively high concentration of the non-SAP and O_3 precursors (NO_x and VOCs). Greater relative levels of these precursors will contribute to relatively more formation of non-SAP and O_3, and therefore relatively less formation of SAP, resulting in a reduced SAP mass fraction and also higher O_3-$PM_{2.5}$ slopes.

The power function coefficient also increased over the past 19 years, from 0.08 in $SP_{NY}1$ to 0.23 in $SP_{NY}4$, indicating the O_3 formation suppression by $PM_{2.5}$ increased for the same $PM_{2.5}$ level from $SP_{NY}1$ to $SP_{NY}4$. It should be noted that there were only four points for the $SP_{NY}4$ fit in Fig. 1b, which could affect the fitted power function coefficient of 0.23. The accuracy of this coefficient was verified for this period by redoing the fitting using $PM_{2.5}$ mass increments of 2 μg m^{-3} (0.23, Supplementary Fig. 1c). The larger fitting coefficient may imply a higher deposition rate of O_3, reactive VOCs, HO_2, and/or NO_x onto $PM_{2.5}$ with a higher non-SAP compared to the same mass concentration with a higher SAP fraction. However, due to the sparsity of detailed measurements and/or directly related confirming studies, it is hard to verify these hypotheses. Due to the simplicity of the non-linear fitting, the empirical power function coefficient determined here may not totally represent the O_3 suppression effect. More studies are warranted for verifying this phenomenon and exploring these explanations further.

Increased O_3–$PM_{2.5}$ relationship in Beijing

$PM_{2.5}$ pollution in Beijing has significantly improved since the clean air action in 2013, with strict emission controls mainly for

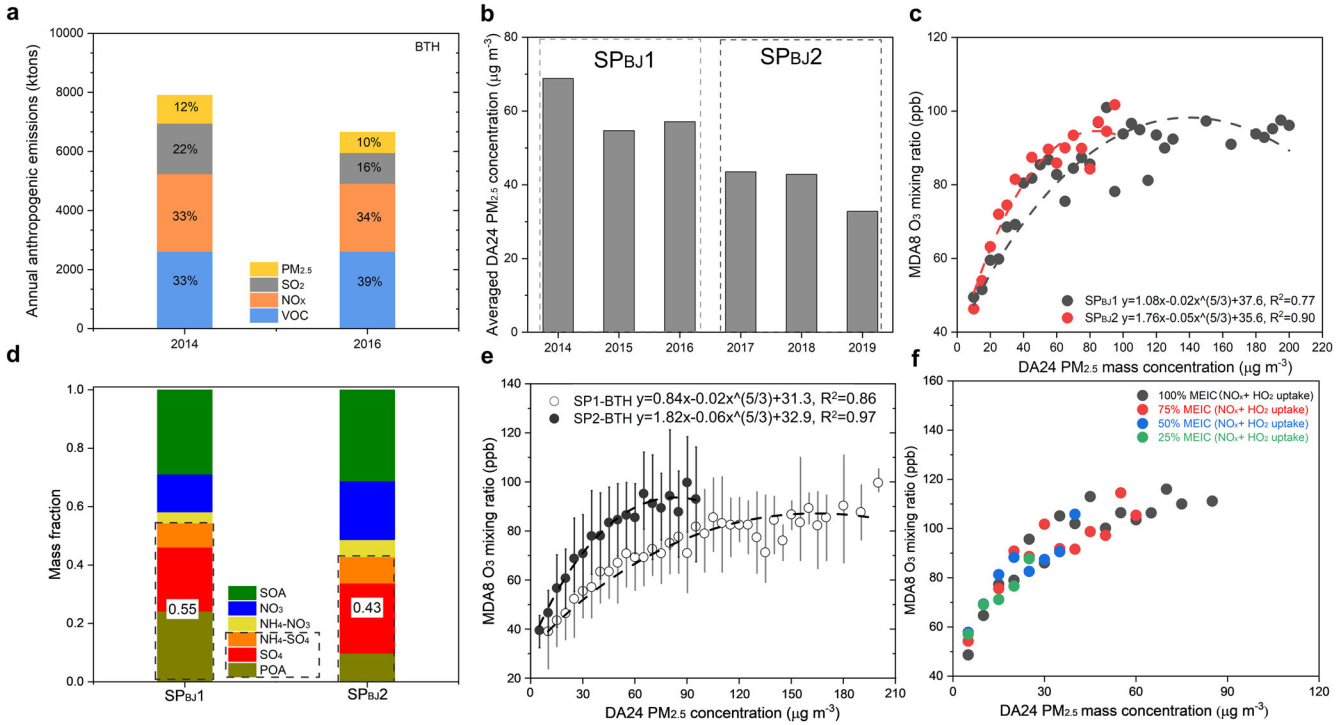

Fig. 2 O_3 and $PM_{2.5}$, and related emissions in Beijing and BTH. a The 2014 and 2016 MEIC anthropogenic emissions in BTH; **b** the time series of the annual summertime average DA24 $PM_{2.5}$ in Beijing for each subperiod specified in the main text; **c** the O_3-$PM_{2.5}$ relationship of Beijing for SP1 and SP2 with the non-linear fitting; **d** the averaged aerosol mass fraction for each subperiod in Beijing. (Black dash box indicates SAP compounds. The number in each column indicates the SAP mass fraction); **e** The O_3 vs $PM_{2.5}$ relationship of main urban cities in BTH for SP1 and SP2 with the non-linear fitting (The error bar indicates 25-75% data range); **f** The O_3 vs $PM_{2.5}$ relationship for different simultaneous emission abatement scenarios based on CMAQ simulations with NO_x and HO_2 uptake for 2017.

SO_2 and primary particle emissions in the Beijing-Tianjin-Hebei (BTH) region (Fig. 2a; see Supplementary Fig. 2 for the location of BTH), yet the region continues to experience elevated O_3 pollution[15–18]. In addition to the fact that emissions of NO_x and VOCs have changed less than $PM_{2.5}$ and SO_2 (a reduction of 12% for NO_x, 0% for VOCs, 28% for $PM_{2.5}$, and 39% for SO_2 comparing 2016 to 2014, Fig. 2a) and remain the major contributor for continued high O_3 concentrations[16,17,21], some alternative explanations for O_3 enhancement include (1) meteorological variability, including elevated temperature, reduced relative humidity (RH) and cloud cover, etc[15,17,22], (2) higher HO_2 concentrations[7] and/or increased photolysis rates[23–25] due to the reduction of particle concentration, and (3) reduced nitrogen oxides (NO_x) emissions[26]. Meanwhile, these emission control policies may also result in a changed summertime O_3-$PM_{2.5}$ relationship such as observed in NYC, which is the focus of this study. To test for this relationship, we separated the time period for Beijing with existing MDA8 O_3 and DA24 $PM_{2.5}$ data (2014-2019) into two subperiods based on the $PM_{2.5}$ concentration – subperiod 1 (hereafter $SP_{BJ}1$, 2014-2016) and subperiod 2 (hereafter $SP_{BJ}2$, 2017-2019, BJ for Beijing), and the standard deviation of the annual summertime average DA24 $PM_{2.5}$ in each period was below 8 μg m^{-3} (Fig. 2b). For each O_3-$PM_{2.5}$ relationship during $SP_{BJ}1$ or $SP_{BJ}2$ (Fig. 2c), in contrast to NYC, there was a fitted MTP with $PM_{2.5}$ mass concentration of about 140 μg m^{-3} for $SP_{BJ}1$ (about 83 μg m^{-3} for $SP_{BJ}2$). However, the existence of the MTP and its location greatly depended on the non-linear fitting, and further studies based on more model simulations and surface observations will help to verify the MTP and reduce the uncertainty of its location caused by the simplicity of the non-linear fitting in this study. Comparing the O_3-$PM_{2.5}$ relationship of Beijing between $SP_{BJ}1$ vs. $SP_{BJ}2$, consistent with the NYC pattern, (1) the O_3-$PM_{2.5}$ linear slope increased from $SP_{BJ}1$ to $SP_{BJ}2$, (2) the power function coefficient increased from 0.02 in $SP_{BJ}1$ to 0.05 $SP_{BJ}2$ indicating the enhanced O_3 suppression by $PM_{2.5}$, and (3) the O_3-$PM_{2.5}$ relationship in $SP_{BJ}1$ and $SP_{BJ}2$ were similar after adjusting for the variability of measured SAP mass fraction in Beijing (Fig. 2d for aerosol composition mass fraction, Supplementary Fig. 3 for O_3-$PM_{2.5}$ non-SAP relationship, and Method 2 for the aerosol composition measurements). The enhanced ($VOCs + NO_x$) emission fraction due to the control policies of $SP_{BJ}2$ is the dominant reason for the increased O_3-$PM_{2.5}$ linear slopes (Fig. 2a), as in NYC. Considering Beijing extreme air pollution episodes as frequently being influenced by regional transport from BTH[27], these O_3-$PM_{2.5}$ relationships in Beijing also represent a regional phenomenon in the BTH region (Fig. 2e) and reflect a complicating consideration in the current regional emission abatements with greater SO_2 and $PM_{2.5}$ reduction.

Regional equal percentage emission reductions

Beijing's $PM_{2.5}$ maximums during $SP_{BJ}2$ are located near the MTP for this period. This implies that it is possible to reduce O_3 and $PM_{2.5}$ together following their relationship line (Fig. 2c, the red line) without encountering the O_3 enhancement that may occur with $PM_{2.5}$ reduction alone. Community Multiscale Air Quality (CMAQ) model simulations (Fig. 2f and Supplementary Fig. 4) verified this possibility by keeping the fraction of each specie emission ($PM_{2.5}$, SO_2, VOCs and NO_x) constant while imposing emission reductions, a strategy named "regional equal percentage emission reductions", which also avoids further increased O_3-$PM_{2.5}$ linear slope observed under the controls targeting mainly SO_2 and $PM_{2.5}$ emissions. As mentioned above, the increased O_3-$PM_{2.5}$ linear slope indicates less O_3 reduction than $PM_{2.5}$ as in NYC. Under regional equal percentage emission reductions, the required BTH regional emission reductions based on the 2019 annual emissions were about (1) 42% to achieve the 2019 Beijing top5% DA24 $PM_{2.5}$ reaching the concentration levels of the 2001

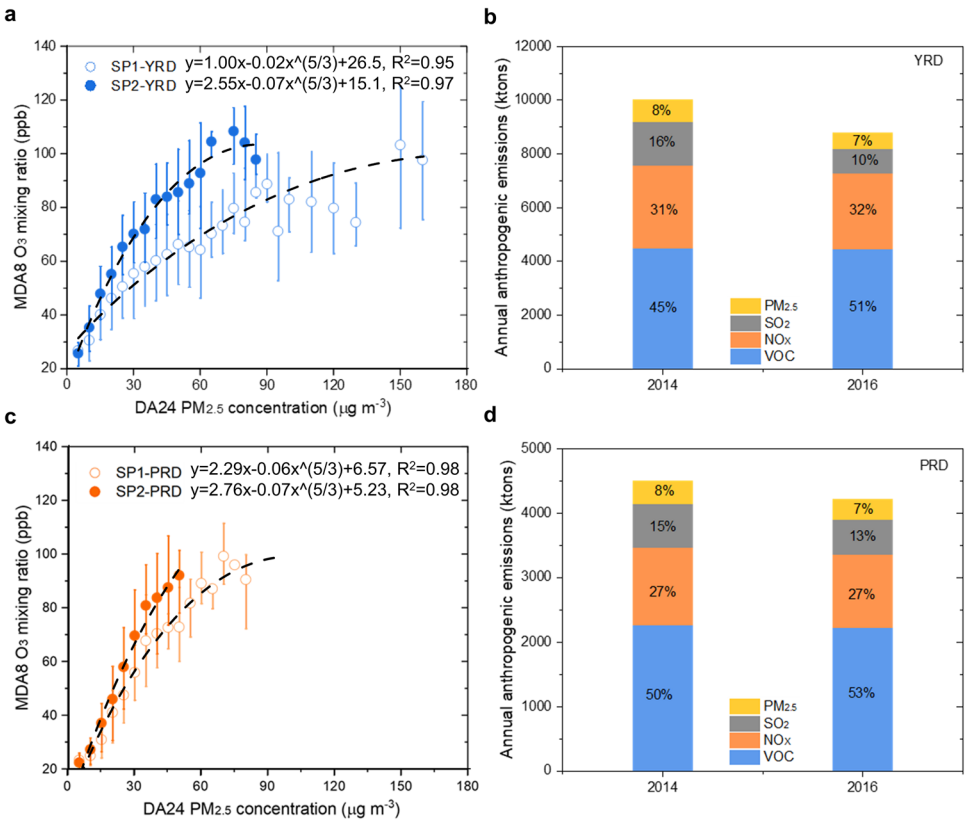

Fig. 3 O_3 and $PM_{2.5}$, and related emissions in YRD and PRD. a The O_3 vs $PM_{2.5}$ relationship of main urban cities in YRD for SP1 (2014–2016) and SP2 (2017–2019) with the non-linear fitting (The error bar indicates 25–75% data range); **b** the 2014 and 2016 MEIC anthropogenic emissions in YRD (including provinces of Shanghai, Jiangsu and Zhejiang); **c** the O_3 vs $PM_{2.5}$ relationship of main urban cities in PRD for SP1 (2014–2016) and SP2 (2017–2019) with the non-linear fitting (The error bar indicates 25–75% data range); **d** the 2014 and 2016 MEIC anthropogenic emissions in PRD (including Guangzhou province).

NYC top5% DA24 $PM_{2.5}$ (39 μg m^{-3}, hereafter "Goal 1"), (2) 53% to reach the MDA8 O_3 concentration below China's O_3 standards (75 ppb, which corresponds to DA24 $PM_{2.5}$ about 29 μg m^{-3} for Beijing, hereafter "Goal 2"), and (3) 70% to reach the 2019 NYC DA24 $PM_{2.5}$ concentration levels (15 μg m^{-3}, hereafter "Goal 3") (Method 4), respectively.

The emission related O_3-$PM_{2.5}$ relationship variations were also observed in two other Chinese megacity clusters, namely the Yangtze River Delta (YRD) and the Pearl River Delta (PRD) (Fig. 3; see Supplementary Fig. 2 for the locations). The O_3-$PM_{2.5}$ linear slope of YRD increased in recent years (Fig. 3a), consistent with the larger reductions in SO_2 and primary $PM_{2.5}$ than non-SAP species (Fig. 3b), with the enhanced O_3 formation suppression by $PM_{2.5}$. To reach the above three goals in Shanghai, the emissions in YRD need to be reduced by 28%, 32%, and 59%, respectively on the basis of the 2019 YRD annual emissions and the Shanghai top5% DA24 $PM_{2.5}$ (Method 4). In comparison, the O_3-$PM_{2.5}$ linear slope of PRD was only slightly increased (Fig. 3c), due to the small changes in emission ratios of SO_2 and $PM_{2.5}$ (Fig. 3d), and the $PM_{2.5}$ suppression effect stayed the same. Meanwhile, the DA24 $PM_{2.5}$ extreme concentration in Guangzhou (representative of PRD) in 2019 was 36.2 μg m^{-3}, which was already below the Goal 1 concentration level. However, additional regional and synchronous emission reductions in PRD by 14% and 69% (Method 4), respectively are needed to meet the other two goals ("Goal 2 and 3").

DISCUSSION

Under current emission policies for NYC and Beijing with larger reductions in the emissions of SO_2 and $PM_{2.5}$ than those of VOCs and NO_x, we obtained an increased O_3-$PM_{2.5}$ linear slope due to the reduced SAP mass fraction, indicating a weaker O_3 reduction than for $PM_{2.5}$. Additional contribution of the increased O_3-$PM_{2.5}$ linear slope can also come from the higher NO_x emission reduction than VOCs (a reduction of 12% for NO_x, 0% for VOCs comparing 2016 to 2014, Fig. 2a), a period during which Beijing was a VOC-limited regime[26]. Regional equal percentage emission reductions could be an achievable way based on CMAQ simulation, to avoid further increased O_3-$PM_{2.5}$ linear slope as are expected under the continuation of current control policies in BTH. We suggest a 42% equal percentage reduction of the BTH emissions as a goal for the 2019 Beijing top5% DA24 $PM_{2.5}$ dropping to the 2001 NYC top5% DA24 $PM_{2.5}$ concentration level (39 μg m^{-3}). Other equal percentage emission controls are needed for other regions to meet pollution reduction goals. We note that equal percentage emission reductions represent only one possible control scenario, and this may not represent an optimal solution Further model simulations with different combinations of NO_x and VOCs emission reductions should be used for future studies to explore the response of the O_3-$PM_{2.5}$ relationship to (1) a range of scenarios, (2) a more accurate non-linear function, and (3) the existence of MTP and its uncertainty, etc.

The suppression of O_3 formation has been described here by a power function whose strength depends on the $PM_{2.5}$ level as shown in Figs. 1 and 2. Mechanistic details of this suppression are not yet known, but there is an indication that it does depend on the chemical composition of the suppressing aerosol. However, it is notable that there seems to have some connection between the variation of the fitted power function coefficient for each city or regions with the O_3–NO_x–VOC sensitivity. These changes in the

fitted power function coefficient during 2014-2019 at BTH (0.02 to 0.06), at YRD (0.02 to 0.07), at PRD (0.06 to 0.08), and during 2001-2019 at NYC (0.08 to 0.23), are consistent with changes in the regime of BTH and YRD transforming from VOC-limited to transitional/weak-VOC-limited, PRD staying at similar transitional/weak-VOC-limited[26,28], and NYC from transitional/weak-VOC-limited to the transitional/weak-NO_x-limited[29]. Thus, it is possible that the power function coefficient varies following the O_3–NO_x–VOC sensitivity, with regions with a power function coefficient of 0.02 in the VOC-limited regime, 0.06 in the transitional/weak-VOC-limited regime, and 0.23 in the transitional/weak-NO_x-limited regime. All of these need to be further verified through more detailed studies. Finally, the emission reduction on NO_x (66% reduction) and VOCs (65% reduction) from NY state comparing 2017 to 2001 could also provide useful guidance for the Chinese megacity clusters, with focusing on the (1) NO_x emission reduction from vehicle emissions, energy generation combustion sources, industrial processes, and (2) VOCs emission reduction from vehicle emissions, solvent utilization, fuel combustion (Supplementary Fig. 5).

METHODS

M1. Non-linear fitting of the O_3-$PM_{2.5}$ relationship

Equation (1) was used in this study to fit the non-linear relationships between O_3 and $PM_{2.5}$, which contains (a) a positive linear part to reflect the O_3/$PM_{2.5}$ co-occurrence[6] without any interaction between these two, (b) a negative power function part reflecting the O_3 formation suppression by $PM_{2.5}$, i.e., the uptake of HO_2/NO_2 by $PM_{2.5}$[7–9] and/or the reduced photolysis rates with $PM_{2.5}$ increasing[20], and (c) a constant. The power function exponent was set to 5/3, based on the considerations of (1) the uptake coefficients of the radicals related to the aerosol surface concentration, proportional to the 2/3 power of $PM_{2.5}$ mass concentration, and (2) the radical concentrations were simply assumed to relate with the O_3 concentration, proportional to the $PM_{2.5}$ mass concentration as mentioned in (a). We ignore the possibility of very high NO concentrations in O_3 formation suppression in this study, based on the linear relationship between MAD8 O_3 and its time-related odd oxidant ($O_x = O_3 + NO_2$) for NYC and Beijing (Supplementary Fig. 6).

$$O_3 = aPM_{2.5} + b(PM_{2.5})^{5/3} + c \quad (1)$$

Where O_3 is its mixing ratio, $PM_{2.5}$ is the its mass concentration, a is the slope of the linear part, b is power function coefficient, and c is the constant. a, b, and c could be fitted through the non-linear fitting of the O_3-$PM_{2.5}$ relationship. It should be noted that Eq. (1) only represents a very simplified solution for the non-linear O_3-$PM_{2.5}$ relationship and will cause some uncertainty for the results. Further studies related to the mechanism are warrantied to explore a more accurate function.

M2. Aerosol chemical composition measurements

The Aerodyne Aerosol Mass Spectrometer (AMS) was used to obtain the chemical composition of non-refractory particulate matter <1 μm in diameter (NR-PM_1). In this study, we assumed that the aerosol composition of PM_1 is similar to $PM_{2.5}$ based on (1) the current application of AMS for PM_1 and $PM_{2.5}$ chemical composition measurements in Beijing with a similar mass fraction[30] and (2) the dominant contribution (>70%) of PM_1 to $PM_{2.5}$ in NYC[31,32] with similar contribution (around 0.7) from each main composition (e.g. sulfate, nitrate, ammonium) of PM_1 to $PM_{2.5}$ comparing the measurements from an AMS to by a Particle-into-Liquid Sampler (PILS) coupled with two Metrohm Compact 761 Ion Chromatography (IC) systems (PILS-IC)[31]. Also, we ignored primary black carbon due to the inability of the standard AMS to detect this species. For NYC, AMS field measurements were made during the summers of 2001[33], 2009[31,34], 2011[35], and 2018[10,32] in NYC or the surrounding area. The aerosol mass fractions of (1) 2001 measurements were used for the subperiod of 2001-2003, (2) the average of 2001 and 2009 for the subperiod of 2004-2008, (3) 2011 for the subperiod of 2009-2013, and (4) 2018 for the subperiod of 2014-2019. For Beijing, AMS measurements were made at the tower branch of the Institute of Atmospheric Physics, a typical urban site located between the north 3rd and 4th ring road in Beijing[36] during 06/07-07/08 in 2014 and 06/01-06/29 in 2017, which were used for the subperiods of 2014-2016 and 2017-2019, respectively. It should be noted that some uncertainties can be caused due to the assumptions used, i.e., the $PM_{2.5}$ mass fraction based on PM_1 measurement, the neglect of primary black carbon, and using a single year for the whole subperiod. Due to the limited measurements, these uncertainties are difficult to fully quantify in this study, and further work could benefit from additional continuous $PM_{2.5}$ composition and other related measurements. The measured OA organic mass spectra have been applied by the Positive Matrix Factorization (PMF) analysis to separate into different OA factors/subtypes[37], such as the oxidized organic aerosols (OOAs) as a surrogate of SOA, and the hydrocarbon-like OA (HOA) as a surrogate of POA[38,39].

M3. Community Multiscale Air Quality model (CMAQ)

The Community Multiscale Air Quality Model (CMAQ) version 5.2 was applied in the current study, coupled with SAPRC-07 mechanism and updated AERO6 aerosol module. The updates including the heterogeneous loss of NO_2, SO_2, glyoxal, and methylglyoxal to form nitrate, sulfate, and SOA. The reactive surface uptake coefficient of NO_2, glyoxal, and methylglyoxal followed Ying et al. (2014)[40] and Ying et al. (2015)[41], respectively and the heterogeneous formation of sulfate from surface-controlled reactive uptake of SO_2 followed Hu et al (2016)[42]. In addition, the uptake of HO_2 onto aerosol surfaces was considered, and an uptake coefficient (γ_{HO2}) of 0.2 was used based on previous studies[6,43–45]. The γ_{HO2} uptake coefficient is related to the aerosol composition, temperature and RH[46], and Tan et al. (2020)[47] showed the impact of aerosol HO_2 uptake effect is much less if a γ_{HO2} of 0.08 was applied in the model, which highlights the large uncertainty for the aerosol HO_2 uptake effect from model simulation using a constant γ_{HO2}. Since our model is mainly used to simulate the effects of emission reductions, rather than focusing on explaining the reason for the increased ozone in China as Li et al (2019)[7] did, and there is good agreement between the observations and the model simulation, it is reasonable to apply γ_{HO2} of 0.2 for this study. The model was applied to simulate O_3 and $PM_{2.5}$ formation during June-August 2017 using a 36 km × 36 km horizontal domain that covers China and surrounding countries in East Asia. The meteorological fields were generated by the Weather Research and Forecasting Model (WRF v4.0.) with a 3D nudging of winds, temperature, and water vapor above the PBL based on the NCEP ADP Global Upper Air Observational Weather Data (https://rda.ucar.edu/datasets/ds351.0/#!access). For anthropogenic emissions, the monthly Multi-resolution Emission Inventory for China (MEICv1.3, https://www.meicmodel.org) and the Regional Emission inventory in Asia (REASv3.1, https://www.nies.go.jp/REAS/) were applied to China and the rest of the domain, respectively. The resolution of both inventories was 0.25°x0.25°. The 2016 MEIC anthropogenic emissions was used for 2017 summertime simulation. Biogenic emissions were generated by the Model for Emissions of Gases and Aerosols from Nature (MEGAN) v2.1, with the leaf area index (LAI) from the 8-day Moderate Resolution Imaging Spectro-radiometer (MODIS) LAI product (MOD15A2) and the plant function types (PFTs) from the Global Community Land Model (CLM 3.0). Open burning emissions were based on the Fire Inventory from NCAR (FINN). Dust and sea salt emissions were

generated via inline processing during CMAQ simulations. Lightning-induced NO_x production was not included in the current study. Initial boundary conditions were based on the default vertical distribution of concentrations provided by CMAQ that represent clean continental conditions with a fixed background O_3 concentration ranges from 30 to 70 ppb. The first 3 days were taken as spin-up days and results were excluded from the analysis. Three days were used based on the consideration that a spin-up time of 48 h would be enough for the chemical components study in the planetary boundary layer[48]. The comparison between the CMAQ simulations and observations for the 24 cities in the BTH and its nearby region are shown in Supplementary Figs. 7–9. In general, the model can well capture the temporal variations of both O_3 and $PM_{2.5}$ in all the cities, with the performance statistics conforming to the recommended benchmarks by Emery et al. (2017)[49] as shown in Supplementary Table 1. Besides the base case with the default emissions of 2016, other cases were designed to represent the possible changes of anthropogenic emissions in the future, including proportional reductions in all the anthropogenic sectors by 25%, 50%, and 75%, respectively.

M4. Synchronous emission reductions estimation

The relationship of top5% DA24 $PM_{2.5}$ concentration with an emission reduction ratio of Beijing (71.6 μg m^{-3}/100% MEIC reduction, Supplementary Fig. 10a) and other cities (75.4 μg m^{-3}/100% MEIC reduction for Shanghai and 34.3 μg m^{-3}/100% MEIC reduction for Guangzhou, Supplementary Fig. 10b, c) from the model simulation was used to estimate the synchronous emission abatements. Meanwhile, the ratios of observed top5% DA24 $PM_{2.5}$ to the simulated values (1.2 for Beijing, 1.0 for Shanghai, and 0.9 for Guangzhou) were used to correct the above estimates, assuming they were within the simulation uncertainty. The corrected estimates were 85.9 μg m^{-3}/100% MEIC reduction for Beijing, 75.4 μg m^{-3}/100% MEIC reduction for Shanghai, and 30.9 μg m^{-3}/100% MEIC reduction for Guangzhou, respectively. The observed 2019 top5% DA24 $PM_{2.5}$ concentration of Beijing (74.8 μg m^{-3}), Shanghai (59.8 μg m^{-3}) and Guangzhou (36.2 μg m^{-3}) were used as the references. The MDA8 O_3 concentration below China's O_3 standards (about 75ppb) related DA $PM_{2.5}$ concentration for Beijing (about 29 μg m^{-3}), Shanghai (about 36 μg m^{-3}), and Guangzhou (about 32 μg m^{-3}) were estimated based on the O_3-$PM_{2.5}$ relations from Figs. 2c, 3a and 3c.

DATA AVAILABILITY

MDA8 O_3, DA24 $PM_{2.5}$ concentration, and pollutants emission inventory sources. Summertime (June-August) 2001–2019, MDA8 O_3 concentrations, and DA24 $PM_{2.5}$ concentrations for the Queens College site were obtained from https://www.epa.gov/outdoor-air-quality-data/download-daily-data. The MDA8 O_3 and daily average $PM_{2.5}$ concentration for summer (June-August) 2014–2019 for Beijing were obtained from the Chinese Ministry of Ecology and Environment (MEE) website (https://english.mee.gov.cn/). The VOCs, NO_x, SO_2 and $PM_{2.5}$ annual emission rates for NYC and NY state were obtained from the EPA National Emissions Inventory website (https://www.epa.gov/air-emissions-inventories/national-emissions-inventory-nei). The AMS measured aerosol chemical composition data for (1) the 2001, 2009, and 2011 NYC field campaigns can be found at https://sites.google.com/site/amsglobaldatabase/, (2) the 2018 NYC field campaign data can be found at https://www-air.larc.nasa.gov/missions/listos/index.html.

Received: 22 March 2022; Accepted: 12 October 2022;
Published online: 04 November 2022

REFERENCES

1. Schnell, J. L. & Prather, M. J. Co-occurrence of extremes in surface ozone, particulate matter, and temperature over eastern North America. *Proc. Natl Acad. Sci. USA* **114**, 2854–2859 (2017).
2. Dear, K., Ranmuthugala, G., Kjellstrom, T., Skinner, C. & Hanigan, I. Effects of temperature and ozone on daily mortality during the August 2003 heat wave in France. *Arch. Environ. Occup. Health* **60**, 205–212 (2005).
3. Willers, S. M. et al. High-resolution exposure modelling of heat and air pollution and the impact on mortality. *Environ. Int* **89**, 102–109 (2016).
4. Zhao, K. et al. A high resolution modeling study of a heat wave-driven ozone exceedance event in New York City and surrounding regions. *Atmos. Environ.* **199**, 368–379 (2019).
5. Zhu, J., Chen, L., Liao, H. & Dang, R. Correlations between $PM_{2.5}$ and ozone over China and associated underlying reasons. *Atmosphere* **10**, 352 (2019).
6. Li, K. et al. A two-pollutant strategy for improving ozone and particulate air quality in China. *Nat. Geosci.* **12**, 906–910 (2019).
7. Li, K. et al. Anthropogenic drivers of 2013–2017 trends in summer surface ozone in China. *Proc. Natl Acad. Sci. USA* **116**, 422–427 (2019).
8. Jacob, D. J. Heterogeneous chemistry and tropospheric ozone. *Atmos. Environ.* **34**, 2131–2159 (2000).
9. Buysse, C. E., Kaulfus, A., Nair, U. & Jaffe, D. A. Relationships between particulate matter, ozone, and nitrogen oxides during Urban smoke events in the Western US. *Environ. Sci. Technol.* **53**, 12519–12528 (2019).
10. Zhang, J. et al. Mobile laboratory measurements of high surface ozone levels and spatial heterogeneity during LISTOS 2018: evidence for sea breeze influence. *J. Geophys. Res. Atmos.* **124**, 1–12 (2020).
11. Sun, Y. et al. Investigation of the sources and evolution processes of severe haze pollution in Beijing in January 2013. *J. Geophys. Res. Atmos.* **119**, 4380–4398 (2014).
12. Wang, J. et al. Fast sulfate formation from oxidation of SO_2 by NO_2 and HONO observed in Beijing haze. *Nat. Commun.* **11**, 2844 (2020).
13. Zhang, Q. et al. Drivers of improved $PM_{2.5}$ air quality in China from 2013 to 2017. *Proc. Natl Acad. Sci. USA* **116**, 24463–24469 (2019).
14. Blanchard, C. L., Shaw, S. L., Edgerton, E. S. & Schwab, J. J. Emission influences on air pollutant concentrations in New York State: I. ozone. *Atmos. Environ.:X* **3**, 100033 (2019).
15. Liu, Y. & Wang, T. Worsening urban ozone pollution in China from 2013 to 2017—Part 1: The complex and varying roles of meteorology. *Atmos. Chem. Phys.* **20**, 6305–6321 (2020).
16. Liu, Y. & Wang, T. Worsening urban ozone pollution in China from 2013 to 2017—Part 2: The effects of emission changes and implications for multi-pollutant control. *Atmos. Chem. Phys.* **20**, 6323–6337 (2020).
17. Li, K. et al. Increases in surface ozone pollution in China from 2013 to 2019: anthropogenic and meteorological influences. *Atmos. Chem. Phys.* **20**, 11423–11433 (2020).
18. Wang, Y. et al. Contrasting trends of $PM_{2.5}$ and surface-ozone concentrations in China from 2013 to 2017. *Natl Sci. Rev.* **7**, 1331–1339 (2020).
19. Seinfeld, J. H. & Pandis, S. N. *Atmospheric Chemistry and Physics: From Air Pollution to Climate Change* 3rd edn (Wiley, 2016).
20. Benas, N. et al. Surface ozone photolysis rate trends in the Eastern Mediterranean: Modeling the effects of aerosols and total column ozone based on Terra MODIS data. *Atmos. Environ.* **74**, 1–9 (2013).
21. Cheng, J. et al. Dominant role of emission reduction in $PM_{2.5}$ air quality improvement in Beijing during 2013–2017: a model-based decomposition analysis. *Atmos. Chem. Phys.* **19**, 6125–6146 (2019).
22. Shi, Z. et al. Sensitivity analysis of the surface ozone and fine particulate matter to meteorological parameters in China. *Atmos. Chem. Phys.* **20**, 13455–13466 (2020).
23. Zhao, S. et al. The influence of aerosols on the NO_2 photolysis rate in a suburban site in North China. *Sci. Total Environ.* **767**, 144788 (2021).
24. Gao, J. et al. The impact of the aerosol reduction on the worsening ozone pollution over the Beijing-Tianjin-Hebei region via influencing photolysis rates. *Sci. Total Environ.* **821**, 153197 (2022).
25. Ma, X. et al. Rapid increase in summer surface ozone over the North China Plain during 2013–2019: a side effect of particulate matter reduction control? *Atmos. Chem. Phys.* **21**, 1–16 (2021).
26. Chen, X. et al. Chinese regulations are working-why is surface ozone over industrialized areas still high? Applying lessons from Northeast US air quality evolution. *Geophys. Res. Lett.* https://doi.org/10.1029/2021GL092816 (2021).
27. Chang, X. et al. Contributions of inter-city and regional transport to $PM_{2.5}$ concentrations in the Beijing-Tianjin-Hebei region and its implications on regional joint air pollution control. *Sci. Total Environ.* **660**, 1191–1200 (2019).
28. Ren, J. & Xie, S. Diagnosing ozone-NO_x-VOC sensitivity and revealing causes of ozone increases in China based on 2013–2021 satellite retrievals. *Atmos. Chem. Phys. Discuss.* https://doi.org/10.5194/acp-2022-347 (2022).
29. Jin, X. et al. Inferring changes in summertime surface Ozone–NO x–VOC chemistry over US urban areas from two decades of satellite and ground-based observations. *Environ. Sci. Technol.* **54**, 6518–6529 (2020).
30. Sun, Y. L. et al. Chemical differences between PM_1 and $PM_{2.5}$ in highly polluted environment and implications in air pollution studies. *Geophys. Res. Lett.* **47**, e2019GL086288 (2020).

31. Sun, Y. L. et al. Characterization of the sources and processes of organic and inorganic aerosols in New York city with a high-resolution time-of-flight aerosol mass spectrometer. *Atmos. Chem. Phys.* **11**, 1581–1602 (2011).
32. Zhang, J. et al. Long Island enhanced aerosol event during 2018 LISTOS: association with heatwave and marine influences. *Environ. Pollut.* **270**, 116299 (2021).
33. Drewnick, F. et al. Measurement of ambient aerosol composition during the PMTACS-NY 2001 using an aerosol mass spectrometer. Part ii: chemically speciated mass distributions. *Aerosol Sci. Technol.* **38**, 104–117 (2004).
34. Sun, Y. L. et al. Factor analysis of combined organic and inorganic aerosol mass spectra from high resolution aerosol mass spectrometer measurements. *Atmos. Chem. Phys.* **12**, 8537–8551 (2012).
35. Zhou, S. et al. Influences of upwind emission sources and atmospheric processing on aerosol chemistry and properties at a rural location in the Northeastern US. *J. Geophys. Res. Amos.* **121**, 6049–6065 (2016).
36. Sun, Y. L. et al. Characterization of summer organic and inorganic aerosols in Beijing, China with an aerosol chemical speciation monitor. *Atmos. Environ.* **51**, 250–259 (2012).
37. Ulbrich, I. M. et al. Interpretation of organic components from Positive Matrix Factorization of aerosol mass spectrometric data. *Atmos. Chem. Phys.* **9**, 2891–2918 (2009).
38. Ng, N. L. et al. Organic aerosol components observed in Northern Hemispheric datasets from Aerosol Mass Spectrometry. *Atmos. Chem. Phys.* **10**, 4625–4641 (2010).
39. Zhang, Q. et al. Understanding atmospheric organic aerosols via factor analysis of aerosol mass spectrometry: a review. *Anal. Bioanal. Chem.* **401**, 3045–3067 (2011).
40. Ying et al. Impacts of Stabilized Criegee Intermediates, surface uptake processes and higher aromatic secondary organic aerosol yields on predicted $PM_{2.5}$ concentrations in the Mexico City Metropolitan Zone. *Atmos. Environ.* **94**, 438–447 (2014).
41. Ying, Q., Li, J. & Kota, S. H. Significant contributions of isoprene to summertime secondary organic aerosol in Eastern United States. *Environ. Sci. Technol.* **49**, 7834–7842 (2015).
42. Hu, J., Chen, J., Ying, Q. & Zhang, H. One-year simulation of ozone and particulate matter in China using WRF/CMAQ modeling system. *Atmos. Chem. Phys.* **16**, 10333–10350 (2016).
43. Xue, L. K. et al. Ground-level ozone in four Chinese cities: precursors, regional transport and heterogeneous processes. *Atmos. Chem. Phys.* **14**, 13175–13188 (2014).
44. Wang, W. et al. Exploring the drivers of the increased ozone production in Beijing in summertime during 2005–2016. *Atmos. Chem. Phys.* **20**, 15617–15633 (2020).
45. Taketani, F. et al. Measurement of overall uptake coefficients for HO2 radicals by aerosol particles sampled from ambient air at Mts. Tai and Mang (China). *Atmos. Chem. Phys.* **12**, 11907–11916 (2012).
46. Thornton, J. A. et al. Assessing known pathways for HO_2 loss in aqueous atmospheric aerosols: Regional and global impacts on tropospheric oxidants. *J. Geophys Res. -Atmos.* **113**, D05303 (2008).
47. Tan, Z. et al. No evidence for a significant impact of heterogeneous chemistry on radical concentrations in the north China plain in summer 2014. *Environ. Sci. Technol. Lett.* **54**, 5973–5979 (2020).
48. Berge, E. et al. A study of the importance of initial conditions for photochemical oxidant modeling. *J. Geophys Res. Atmos.* **106**, 1347–1363 (2001).
49. Emery, C. et al. Recommendations on statistics and benchmarks to assess photochemical model performance. *J. Air Waste Manag. Assoc.* **67**, 582–598 (2017).

ACKNOWLEDGEMENTS

The authors acknowledge support from the New York State Energy Research and Development Authority (NYSERDA, contract no. 48971), the National Natural Science Foundation of China (no. 42021004), the National Key Research and Development Program of China (no. 2018YFC0213802). We acknowledge the free use of ozone and $PM_{2.5}$ data from the US EPA and China's Ministry of Ecology and Environment. Special thanks to Prof. Daniel J. Jacob from Harvard University for providing valuable comments for this study.

AUTHOR CONTRIBUTIONS

J.Z., J.W. and J.S. designed the research and led the writing, J.Z., Y.S., and W.X. performed experiments, J.L. performed the CMAQ model simulation, J.Z., J.W., Y.S. and J.L. analyzed the data, M.N., J.Y., K.L., B.C., J.M., M.J.S., W.L., X.G., M.C., Q.Y., and Q.Z. contributed significant comments and editing of the paper.

COMPETING INTERESTS

The authors declare no competing interests.

ADDITIONAL INFORMATION

Supplementary information The online version contains supplementary material available at https://doi.org/10.1038/s41612-022-00309-8.

Correspondence and requests for materials should be addressed to Jie Zhang, Junfeng Wang or James J. Schwab.

Reprints and permission information is available at http://www.nature.com/reprints

Publisher's note Springer Nature remains neutral with regard to jurisdictional claims in published maps and institutional affiliations.